Pergamon

Cement and Concrete Research 32 (2002) 1673–1675

CEMENT AND CONCRETE RESEARCH

Communication

X-ray microtomography (microCT) of the progression of sulfate attack of cement paste

S.R. Stock[a,*], N.K. Naik[b], A.P. Wilkinson[c], K.E. Kurtis[b]

[a]*School of Materials Science and Engineering, Georgia Institute of Technology, Atlanta, GA 30332-0245, USA*
[b]*School of Civil and Environmental Engineering, Georgia Institute of Technology, Atlanta, GA 30332-0245, USA*
[c]*School of Chemistry and Biochemistry, Georgia Institute of Technology, Atlanta, GA 30332-0245, USA*

Received 10 December 2001; accepted 3 April 2002

Abstract

High-resolution X-ray computed tomography (i.e., microCT or microtomography) was used to study the sulfate attack of cylinders of Type I cement paste cast with water–cement (w/c) ratios of 0.45, 0.50 and 0.60. Damage levels in samples exposed to a Na_2SO_4 solution with 10,000 ppm sulfate ion concentration were qualitatively rated from 0 (*no damage*) to 4 (*extreme damage*) based upon visual examination of the samples' exteriors and microtomography of the samples' interiors. The greater the w/c ratio, the more rapid the onset of sulfate damage. The corners of the cylinders appeared to be particularly susceptible to spalling, and damage may have continued into the cement paste by formation of subsurface cracks.

Keywords: Microtomography; MicroCT; Cement paste; Sulfate attack; X-ray; Nondestructive evaluation

1. Introduction

Deficiencies exist in the current understanding of sulfate attack reaction kinetics and damage mechanisms in Portland cement [1,2], and this prevents rational design for long-term durability in sulfate environments. Existing standard test methods have been criticized for not reliably predicting performance. For the most sensitive and critical of applications—concrete containment vessels—these deficiencies become safety issues. For more typical applications, such as hydraulic structures or housing, these deficiencies are economic and environmental sustainability issues.

In materials as complex and highly variable as concrete (or one of its constituents, Portland cement paste), enormous advantages accrue if individual samples can be examined nondestructively multiple times during the course of environmental attack. X-ray computed tomography is one of the few ways of doing this, and microtomography (i.e., very-high-resolution X-ray computed tomography) allows the internal structure of optically opaque samples to be imaged with spatial resolution approaching that of optical microscopy. This paper describes preliminary data for Type I cement paste samples subjected to sulfate attack, i.e., to demonstrate applicability of microtomography and to define sampling intervals during sulfate exposure for subsequent series of specimens.

2. Background

X-ray computed tomography employs a set of views through the sample (i.e., projection radiographs taken along different directions) and mathematically recombines them into a cross-sectional map of the X-ray absorptivity. The spatial frequencies and contrast present in the projections (spatial sampling) and the number of projections (angular sampling) define maximum spatial resolution and contrast sensitivity, which can be present in the reconstructed images. As a rule of thumb, a 1000 element X-ray detector can reconstruct a 10-mm object with physically meaningful isotropic volume elements (voxels) no smaller than 10 μm.

* Corresponding author. Present address: Institute for Bioengineering and Nanoscience in Advanced Medicine, Tarry 16-717, Northwestern University, 303 East Chicago Avenue, Chicago, IL 60611-3008, USA. Tel.: +1-847-917-7273; fax: +1-312-503-2544.

E-mail address: s-stock@northwestern.edu (S.R. Stock).

0008-8846/02/$ – see front matter
PII: S0008-8846(02)00814-1

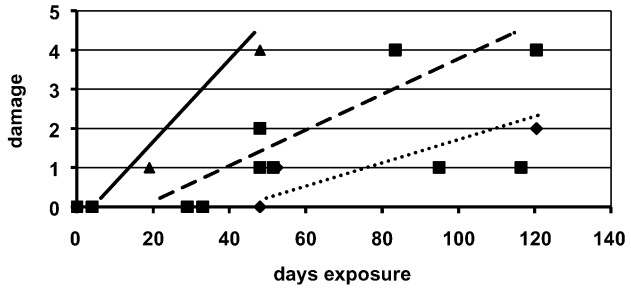

Fig. 1. Qualitative estimates of damage as a function of sulfate exposure, with 0 denoting *no damage* and 4 *extreme damage*, for w/c ratios of 0.6 (triangles, solid line), 0.50 (squares, dashed lines) and 0.45 (diamonds, dotted line).

Prior microtomography studies of evolving structural materials include damage of metal matrix composites accompanying mechanical testing [3–5] and 3D patterns of crack face contact in situ and for different loads in aluminum samples [6,7]. Concrete has also received attention [8–11]. Further information on computed tomography appears elsewhere [12–14].

3. Materials and methods

Cylindrical samples of Type I cement (ASTM C 150-00 [15]) were cast in plastic molds for 24 h, and three water–cement (w/c) ratios were investigated: 0.45, 0.50 and 0.60 by weight. After removal from the mold, the ~10-mm-diameter, ~40-mm-long samples were cured in a lime bath for 3 days or longer (up to 8 days in some cases). After rinsing, the samples were placed in a Na_2SO_4 solution (10,000 ppm sulfate ion concentration) and, after each increment of exposure, the progress of sulfate attack was monitored visually and by microtomography using a Scanco MicroCT-20 or a MicroCT-40 system typically using 500 projections of 0.35 s integration time, 1024 samples/projection, 70 kVp X-rays, 20 μm in-plane voxels and 30 μm slice thickness.

4. Results and discussion

Fig. 1 shows the progression of damage with sulfate exposure using a scale of 0 (*no damage*) to 4 (*extreme damage*), i.e., the qualitative damage level as a function of sulfate exposure time for the three w/c ratios studied. The lines have been added only to guide the eye and are not intended to imply a functional relationship. Three damage states (1, 2 and 3) are illustrated by 3D renderings (produced by Scanco software) of cement paste samples (Fig. 2). These data show that the sulfate attack, consisting of cracking and eventual surface spalling, proceeds most rapidly for the 0.6 w/c samples and most slowly for the 0.45 w/c samples. The greatest part of the scatter in Fig. 1 relates to the crude damage scale and simplistic application; some relate to experimental factors left uncontrolled (differences in curing times, solution agitation, etc.). Nonetheless, the data serve to paint a broad-brush picture of the rate and morphology of attack for the conditions investigated.

Cracks originate near the corners of the cylinders. The proximity of the two surfaces (cylinder top and side) may allow reactants to build to a critical level most rapidly at the corners; alternatively, the minimal constraint at the corners localizes crack initiation. The effect of the corners becomes more pronounced as environmental attack continues; the end of the cylinders eventually become rounded as material spalls from the surface. Slices acquired prior to the onset of cracking reveal that the initial crack geometry and subsequent spalling do not have an origin as subsurface casting defects with dimensions greater than a few tens of micrometers in cross-section and perhaps 5 μm in thickness. Later, however, subsurface cracks appear to form in response to the continuing sulfate attack (middle, Fig. 2), but microtomography data at higher temporal resolution are required to clarify the role of these late-developing cracks.

5. Conclusions

For cement paste samples, the greater the w/c ratios (at least between 0.45 and 0.6), the more rapid the onset of

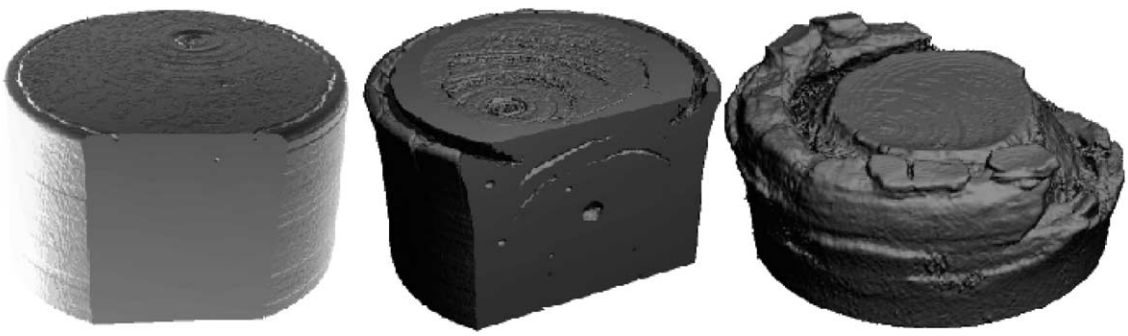

Fig. 2. Microtomography-based 3D renderings of damaged cement paste samples with damage levels 1 (w/c 0.45), 2 (w/c 0.50) and 3 (w/c 60), left to right, respectively.

sulfate damage. The corners of the cylinders appeared to be particularly susceptible to spalling, and X-ray microtomography was instrumental in revealing details of subsurface damage progression.

Acknowledgments

The research was supported by NSF CMS grant 0084824, and data were collected at the Georgia Tech Microtomography Facility supported by NSF BES grant 9977551.

References

[1] P.K. Mehta, Sulfate attack on concrete—a critical review, Materials Science of Concrete, vol. III, American Ceramic Society, Westerville, OH, USA, 1992, pp. 105–130.
[2] M. Santhanam, M.D. Cohen, J. Olek, Sulfate attack research—wither now? Cem. Concr. Res. 31 (2001) 845–851.
[3] J.H. Kinney, S.R. Stock, M.C. Nichols, U. Bonse, T.M. Breunig, R.A. Saroyan, R. Nusshardt, Q.C. Johnson, F. Busch, S.D. Antolovich, Nondestructive investigation of damage in composites using X-ray tomographic microscopy, J. Mater. Res. 5 (1990) 1123–1129.
[4] T.M. Breunig, Nondestructive evaluation of damage in SiC/Al metal/matrix composite using X-ray tomographic microscopy, PhD Thesis (supervised by S.R. Stock), Georgia Institute of Technology, 1992.
[5] T.M. Breunig, S.R. Stock, A. Guvenilir, J.C. Elliott, P. Anderson, G.R. Davis, Damage in aligned fibre SiC/Al quantified using a laboratory X-ray tomographic microscope, Composites 24 (1993) 209–213.
[6] T.M. Breunig, S.R. Stock, S.D. Antolovich, J.H. Kinney, W.N. Massey, M.C. Nichols, A framework relating macroscopic measures and physical processes of crack closure of Al–Li alloy 2090, Fracture Mechanics: Twenty-Second Symposium, Vol. 1, ASTM Spec. Tech. Publ. 1131 (1992) 749–761.
[7] A. Guvenilir, T.M. Breunig, J.H. Kinney, S.R. Stock, New direct observations of crack closure processes in Al–Li 2090 T8E41, Philos. Trans. R. Soc. London 357 (1999) 2755–2775.
[8] I.L. Morgan, H. Ellinger, R. Klinksiek, J.N. Thompson, Examination of concrete by computerized tomography, J. Am. Concr. Inst. 77 (1) (1979) 23–27.
[9] H.E. Martz, D.J. Schnebeck, G.P. Roberson, P.J.M. Monteiro, Computerized tomography analysis of reinforced concrete, ACI Mater. J. 90 (1993) 259–264.
[10] S.P. Shah, S. Choi, Nondestructive techniques for studying fracture processes in concrete, Int. J. Fract. 98 (1999) 351–359.
[11] E.N. Landis, D. Keane, X-ray microtomography for fracture studies in cement-based materials, Developments in X-ray Tomography II, SPIE Proc. vol. 3772 (1999) 105–113.
[12] Industrial Computed Tomography Topical Proceedings (1989); Industrial Computed Tomography II Topical Proceedings (1991), ASNT, Columbus, OH.
[13] S.R. Stock, Microtomography of materials, Int. Mater. Rev. 44 (1999) 141–164.
[14] Developments in x-ray tomography, SPIE Proc. 3149 (1997); Developments in x-ray tomography II, SPIE Proc. 3772 (1999).
[15] Standard Specification for Portland Cement, ASTM C150-00.